PSR J1723-2837: Intensive photometric study captured unique events.

Andre van Staden
South Africa

andre@etiming.co.za

Abstract: PSR J1723-2837, a 1.86 millisecond pulsar (MSP) is one of the growing populations of MSP pulsars with a non-degenerative companion star of mass 0.2 – 0.4 M⊙, also known as Redbacks (RBs), in a ~15 hour orbital period. The presented paper reports on photometric results obtained on the ~16 magnitude companion to PSR J1723-2837. The optical light curve of the companion was intensively monitored for a period of one year.

A steady state was identified, dominated by ellipsoidal variation, a common signature to a number of RBs followed by a transitional period of asymmetric phase luminosity during 2014. Most unexpectedly was the development of a presumably asynchronous rotating spot in 2015 which was observed until the end of 2015 when observations ceased.

1 Introduction

PSR J1723-2837 is an eclipsing, 1.86 MSP in an almost circular ~14.8 hour orbit, about a companion star (J17232318-2837571) of spectral type G5 that was identified using Infrared, optical, ultraviolet and spectrophotometry in previous studies [Crawford, 2013]. X-Ray emission was also detected from PSR J1723–2837 and is presumably a candidate for a radio pulsar/X-ray binary transition object [Bogdanov, 2014].

PSR J1723-2837 is likely a RB system with a heavy companion mass range of 0.4 to 0.7 M⊙ and an orbital inclination angle range of between 30° and

41°, assuming a pulsar mass range of 1.4−2.0 M⊙ [Crawford, 2013], [Roberts, 2012].

Time series photometry on RBs and Black Widows (BW), similar to RBs but with a lighter companion star, M <<0.1 M⊙, are generally time constrained where vital information is recovered, for example identifying the associated companion, revealing light curve properties, Spectral analyses, etc. J1723-2837 has an optical companion of ~16mag allowing favourable photometric opportunities for even small telescopes. In this context, the focus of this study was to monitor the light curve behaviour over a period of one year.

The source of optical emission from BWs and RBs are produced by the companion star. Due to the gravitational pull of the MSP, the companion star becomes tidally distorted. The apparent geometry as seen from Earth is constantly changing while orbiting because the companion is tidally locked to the MSP. This in turn produces ellipsoidal variations in the light curve with two peaks ($4\pi\cdot\phi$). The maximum light received is when the maximum areas are exposed, i.e. when we see the side of the star at ϕ = 0.0 and ϕ = 0.5. Minimums are expected at ϕ = 0.25 and ϕ =0.75 at inferior/superior conjunction when viewing the smaller surfaces and where the effects of gravity and limb darkening also contributes to the weaker flux received.

Irrespective of the ellipsoidal variation, the majority of BWs shows a single-peak ($2\pi\cdot\phi$) optical light curve [e.g., Stappers et al. 2001], with the peak around ϕ = 0.75. This is believe to be a consequence of the heating of the companion star surface, due to irradiation of relativistic photons and/or high energy particles from the MSP [Breton et al. 2013].

Examples of RBs with single-peak light curves [Salvetti et al. 2015] are: PSR J1023+0038 [Thorstensen & Armstrong 2005], J2215+5135 [Schroeder & Halpern 2014], J2339−0533 [Romani & Shaw 2011], and J1227−4853 [Bassa et al. 2014], while examples of RBs with double-peaked light curves

are: PSR J1628−3205 [Li et al. 2014], J1816+4510 [Kaplan et al. 2012] and J2129−0428 [Hui et al. 2015].

2 Observations

2.1 Statistics

Observational period: 3 August 2014 – 16 October 2015
Observational nights: 67
Total observational time: ~260 hours
Total number of photometric measurements: 2000+.

A graphical representation of observations made was presented in Figure 1 showing consecutive groups ranging from GR1 to GR14. A summary of the groups can also be found in Table 2.

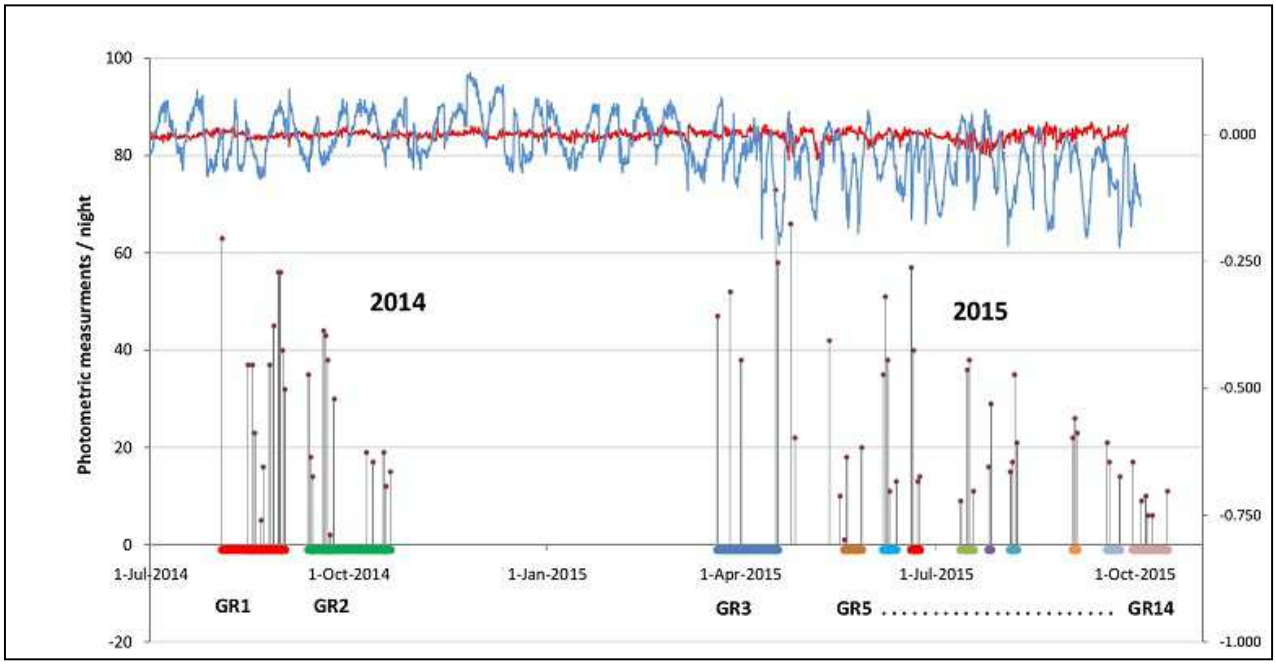

Figure 1**.** *Graphical representation of observations made for this report. The blue and red curve shows a series plot of all photometric data for J1723-2837 and a close-by comparison star respectively (not plotted to time). The Stem plot shows the distribution, number of photometric measurements and how the data was grouped*.

2.2 Observations and data analysis

All observations were obtained from the authors site (International observatory code 641 – Overberg, South Africa) with a 30 cm SCT and ST9e CCD (512x512) cooled to -15 °C. The site experiences minimal light pollution and has seeing with FWHM normally between 2 to 3 arcsec, occasionally reaching < 2 and >3 arcsec. No light filters were used. Light exposures were all 300 seconds in 2014 and were increased to 600 seconds during 2015. The increased integration time resulted in marginal improvement with negligible effect overall. J1723-2837 was located and identified from coordinates and an image by the WIYN 0.9-m telescope [Crawford, 2013].

Photometric measurements for J1723-2837 in this report are based on differential (V-C) magnitudes, computed with Muniwin 2.0.17, a public photometric program. A set of six comparison stars in the FOV were cautiously selected to compute a virtual comparison star (C) for the V-C computation. A comparison star was plotted in a number of figures in this report and was selected as a variable from the group of six (comparison) stars. A standard deviation of 0.009 mag was calculated for the comparison star with no long term deviations. A Lomb-Scargle analysis on the comparison star showed good distribution of energy in the frequency range. The possible effect of mass extinction due to unfiltered images was extensively investigated and found to be negligible on the results reported in this article.

Timing for CCD images was derived from PC time, synchronized to an international time server with additional spot checks against a GPS Master clock. The camera software converts PC system time to mid-exposure time in UT. Muniwin performs heliocentric correction on UT. All photometric measurements in this report referred to heliocentric time.

2.3 Conventions

Magnitude scale: Phase plots were expressed in flux and is related to magnitude with the relationship; Flux = -(V-C) + offset, where V-C is the

differential photometric magnitude and offset was calculated as the mean value of the ellipsoidal signal in order to bring the signal to centre zero. Therefore, more positive flux corresponds to brightening of an object where flux in the negative direction means dimming of the object.

Phases of the companion star: Phase orientation was adopted to be consistent with the radio ephemeris for PSR J1723-2837 [Crawford et al. 2013, Tab. 3] with primary intervals:

ϕ = 0.00: The time of ascending node (MJD 55425.320466), the epoch of phase zero. The companion is approaching us with maximum velocity according to **Doppler measurements [Crawford et al. 2013].**

ϕ = 0.25: This interval encompasses the inferior conjunction where the pulsar is behind its companion and where radio eclipses were observed from the pulsar [Crawford et al. 2013].

ϕ = 0.50: Viewing the companion from the long-axis side (same as ϕ = 0.00). **This is also the trailing (receding) side of the companion.**

ϕ = 0.75: The pulsar is between the companion and earth. Irradiation from pulsar heat is expected to play an important role at this orientation.

The period for the phase plots included the 1st and 2nd orbital period derivate and phases (ϕ_t) were calculated for mid-times of exposures with the relation,

$$\phi_t = \left(T_{asc} \cdot f_b\right) + \left(T_{epoch} \cdot \dot{f}_b\right) + \left(\frac{T_{epoch}^2 \cdot \ddot{f}_b}{2}\right)$$

Where T_{asc} is the time interval starting at the time of ascending node (MJD 55425.320466) and T_{epoch} is the time interval starting at the time of

Epoch (MJD 55667). Orbital derivatives were selected from Table 1. All observational times were Heliocentric corrected.

3 Results

3.1 Ellipsoidal variation – (Group 1 & 3)

The companion to J1723-2837 shows a double peaked light curve signal dominated by ellipsoidal variations of 0.108 magnitudes. A nominal light curve (Figure 2- left) was defined based on data consistently stable, following the ellipsoidal patterns based on 17 observational nights consisting of groups 1 and 3.

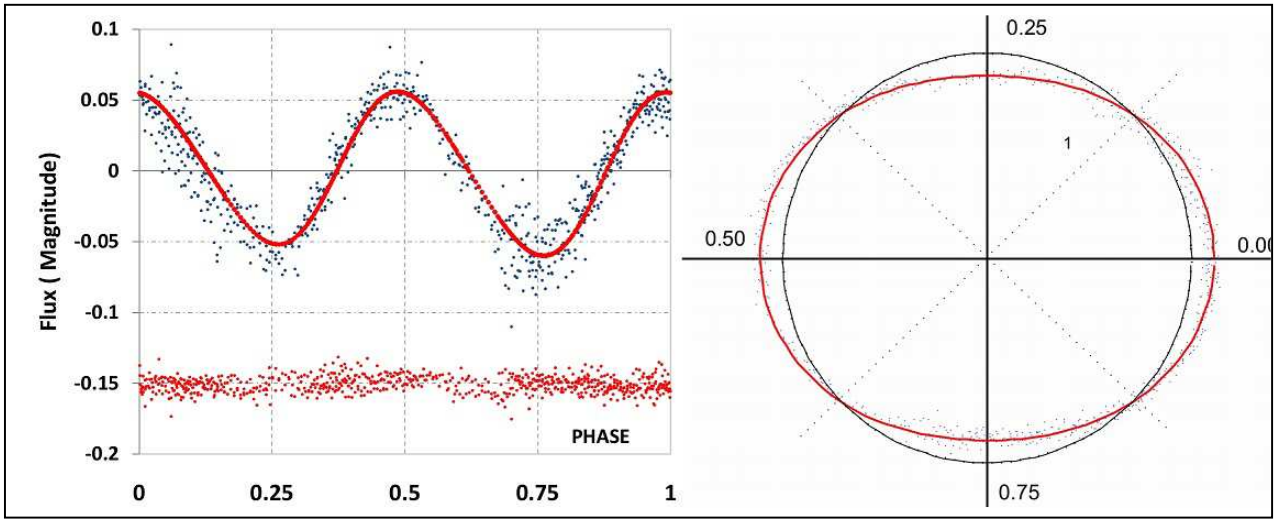

Figure 2**.** (Groups 1 & 3) Folded phase plots for J1723-2837 and comparison star (red dots below). The red curve represents the nominal ellipsoidal signal. The ellipse on the right represents the same nominal light curve as a polar plot. (A radius magnitude of one unit was added for demonstration purposes)

Evidently from the phase plot is the unequal minima at ϕ = 0.25 and ϕ = 0.75. Phase = 0.75 is slightly dimmer compare to ϕ = 0.25. This occurrence was also observed in other RB studies. e.g.: PSR J1628−3205 [Li et al. 2014], J2129−0428 [Hui et al. 2015], J1824-2452H [Pallanca et al. 2010]. Apart from this, the data shows an overall good symmetry as presented with the polar phase plot in the right panel, Figure 2 (red ellipse). Although

relatively small, minor variations were seen in the data during this period particularly from ϕ = 0.75 to ϕ = 0.25. The data from group 1 matched the data from group 3 excellently, confirming observations to be consistent beween 2014 and 2015 with no measurable change in magnitude.

3.2 Asymmetric maximum – (Group 2)

During September 2014, a sudden increase in luminosity was observed in the ϕ = 0.5 region of ~0.04 mag as shown here in Figure 3. This episode was observed until the 20 October, 2014 when observations were stopped due to low altitude angles.

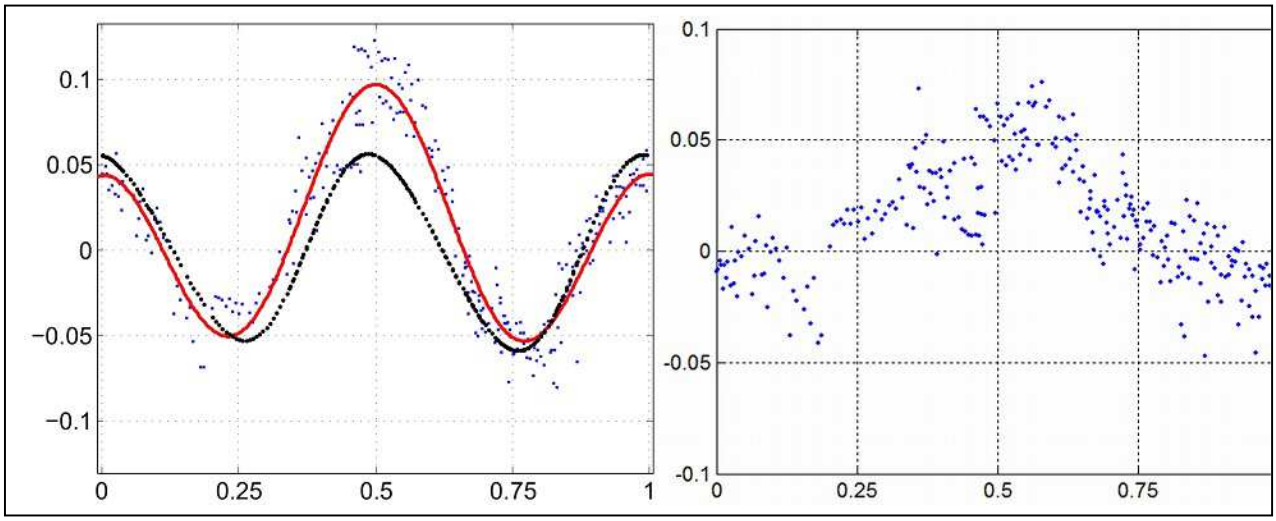

Figure 3**.** *(Group 2) The red curve fitted to the data shows the deviation from the nominal signal plotted in black, during the mentioned period. The plot on the right shows the differences between the two signals.*

3.3 Photometric dips (Groups 5 to 14)

Observations made from May 2015 to October 2015 revealed another episode of large variations as shown in Figure 4.

The data was analysed by first removing the nominal ellipsoidal signal. The resulting signal was still heavily convolved in both phase and amplitude, evident from phase diagrams and Fourier analyses. However, by carefully dividing the data in smaller consecutive groups (GR 5 - GR 14) consisting of

observations closely spaced, resolved events are seen as dips in the light curve data. See Figures 7 to 16 at the end.

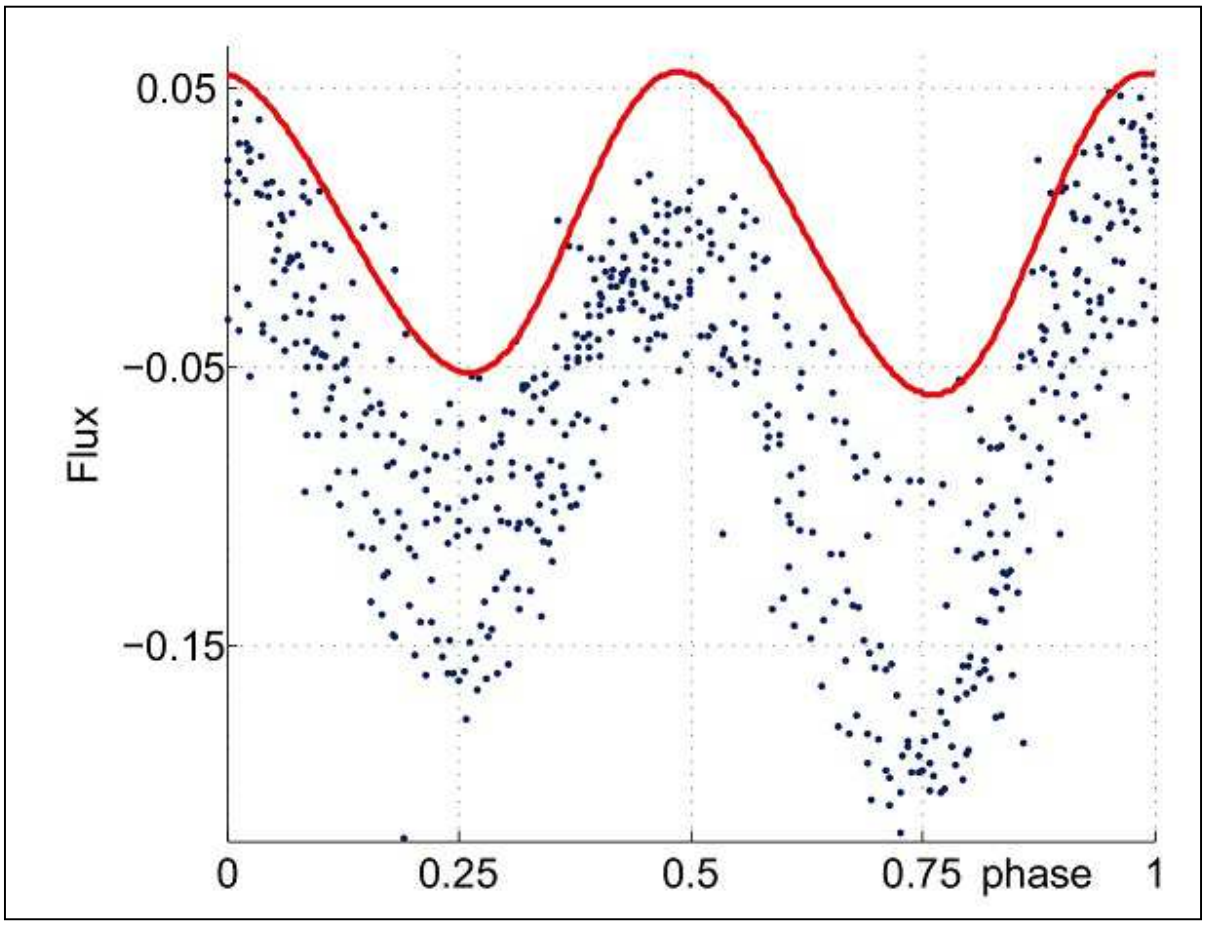

Figure 4*. (Groups 5 to 14) Data captured during May 2015 to October 2015 shown here with blue dots and a nominal ellipsoidal signal plotted in red.*

From the observed ellipsoidal variation we believed that the companion star is tidally locked to the NS or least geometrically fixed. In this case, the companion star co-rotates (geometrically) with the rotating frame induced by orbital rotation and we can therefore describe longitudinal events on the star in terms of phase measurements.

In this context, the first observed dip (GR 5) is coincident with $\phi \sim 0.75$ which can be related to a position on the star, for instance a cold spot on

the surface at that particular longitudinal position. All consecutive dips or cold spots were measured in this fashion including phase error estimations

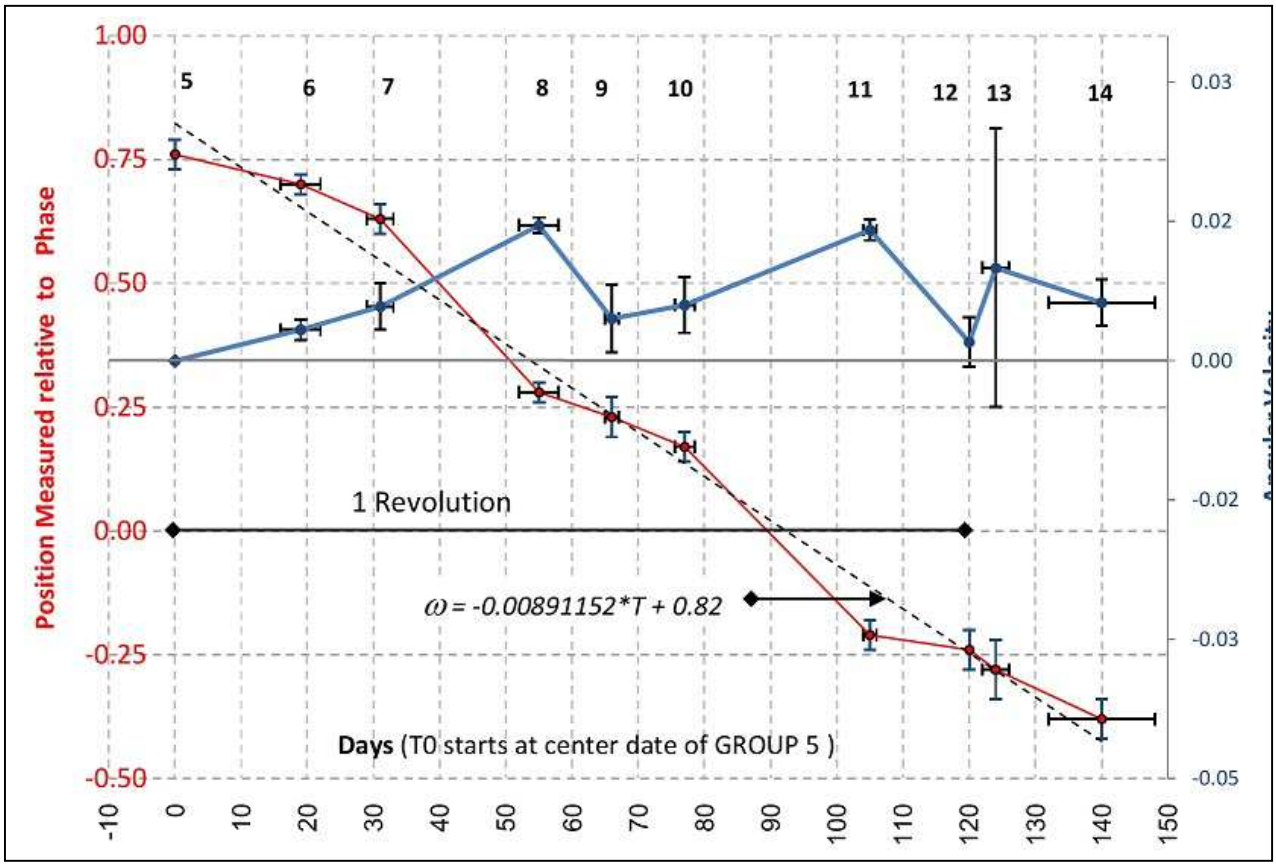

Figure 5**:** *The red dots represent the measured longitudinal positions from Group 5 to 14. Horizontal error bars indicate the corresponding group period. For vertical bar estimations, see figures 7-16. Blue dots represent the corresponding angular velocity. Velocity vertical error bars were derived from the phase errors. Note that phase -0.25 is the same as phase 0.75.*

Most notable in this arrangement is the shifting of phase in one direction at a near constant rate which strongly relates to the effect of angular rotation. In this scenario we can imagine a rotating star with a single spot observed at different times. In support of this idea, the shape and size of the dip remain reasonably constant throughout the full period. From the spot movement we calculated an average rate $\omega = d\varphi/dt$ of 0.008911/day (see dotted line) indicating a rotation period of 112 days while the true

period for one revolution took approximately 120 days. The discrepancy lies in the small deviations from the mean, probably caused by brief periods of deceleration and acceleration in angular rotation. A second curve, although very crude, shows this effect as an angular velocity $\omega = d\varphi/dt$ between consecutive spots. Remarkable is the steady increase in velocity from the start at $\phi \sim 0.75$. e.g. a spin-up scenario. Similarly, there may have been brief periods of deceleration and acceleration in the region at $\phi \sim 0.25$ and again at $\phi \sim 0.75$.

From the onset of this episode, the companion star suddenly dropped 0.05 magnitudes in luminosity in contrast to a stable period since 2014. The dip sizes covered approximately 60% of the phase and slightly increased after 120 days. (see Table 2).

Two minor disturbances were also detected which may be additional cold spots or merely distortion of main spot. These minor events lag the main spot respectively by 0.28 and 0.60 in phase. Although this observation may be important, the effect on the presented phase position measurements was negligible. For completeness, Figure 6 was created to illustrate the effect of the first event.

4 Discussion

J1723-2837 is one of the heaviest RBs and closest to Earth with an optical companion of ~16mag allowing favourable photometric opportunities. The companion star was observed for more than 260 hours in its ~15 hour orbit for a period of one year. Detailed attention was given to the integrity of the data.

The companion star shows a very distinct double peak light curve signal dominated by ellipsoidal variations. A nominal light curve with good precision was established therefore providing a free parameter value for further modelling. No irradiation was observed at $\phi = 0.75$, in fact it was shown that the phase at 0.75 measured slightly dimmer compare to the

phase at 0.25. The weaker flux at phase 0.75 is often explained as a contribution to the effects of gravity and limb darkening. Interestingly, it seems so far from available data that all of the heavier RB companions (Mc > ~0.2M) shows a double peak light curve with absence of irradiation while the ligter systems and BWs show strong irradiation induces curves.

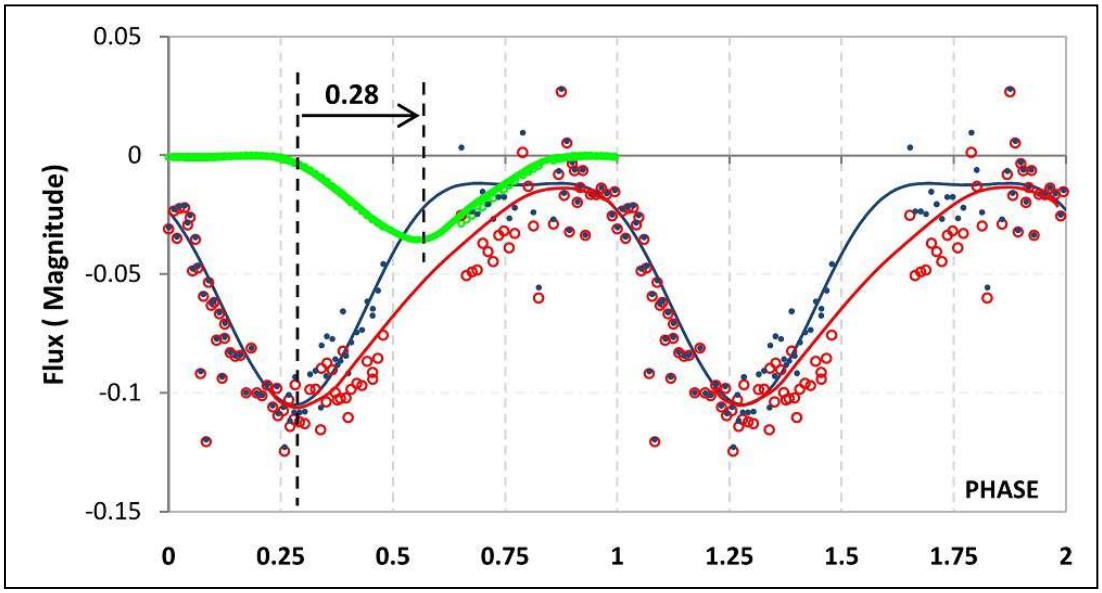

Figure 6*: Data from GROUP 8: The measured data (red dots) shows a slightly asymmetrical dip. Assuming a second minor dip (green curve) was responsible for the deformation and applying this (inverted) to the data we see a reasonable symmetrical correction as illustrated with the blue dots.*

During September 2014, a sudden increase in luminosity was observed in the ϕ = 0.5 region, proceeding for more than two months. Asymmetric peaks, particularly, $\phi_{0.5} > \phi_{0.0}$ is not an uncommon manifestation and were observed in a number of RBs. We noticed that J1723-2837 changes from $\phi_{0.5} \approx \phi_{0.0}$ to $\phi_{0.5} > \phi_{0.0}$ and back to $\phi_{0.5} \approx \phi_{0.0}$.

Most unexpectedly was the development of a presumably asynchronous rotating spot in 2015 which was observed until the end of 2015 when observations ceased. Spots have not been observed in MSP companions to date nor is there evidence for angular rotation. However, they may have been missed up to now because of insufficiently continuous observations.

Magnetic activity is a likely candidate when it comes to explaining star spots, however it will be exciting, though unique, if J1723-2837 showed signs of reverse flow of accreting material through the L1 point. In this scenario an influx of cooler material from a previous accreting phase will cause the star to contract and spin up to conserve angular momentum while keeping the filling factor well below the Roche overflow limit for a period of time. Occasionally, larger clumps of in-falling material will produce a cold spot before contracting and starts to rotate.

References

Bassa, C. G., Patruno, A., Hessels, J. W. T., et al., 2014, *MNRAS*, **441,** 1825

Bogdanov S., et al., 2014, *ApJ*, **781**, 6

Breton, R. P., van Kerkwijk, M. H., Roberts, M. S. E., et al., 2013, *ApJ*, **769,** 108

Crawford F., et al., 2013, *ApJ*, **776**, 20

Hui, C. Y., Hu, C. P., Park, S. M., et al., 2015, *ApJL*, 801**,** 27

Kaplan, D. L., Stovall, K., Ransom, S. M., et al., 2012, *ApJ*, **753,** 174

Li, M., Halpern, J. P., Thorstensen, J. R., 2014, *ApJ*, **795,** 115

Pallanca, C., et al., 2010, ArXiv e-prints, *arXiv*:1010.2661v1 [astro-ph.SR]

Roberts, Mallory S. E., 2012, ArXiv e-prints, *arXiv*:1210.6903v2 [astro-ph.HE]

Romani, R. W. & Shaw, M. S., 2011, *ApJ*, **743**, L26

Salvetti,D., et al., 2015, ArXiv e-prints, *arXiv*:1509.07474v2 [astro-ph.HE]

Schroeder, J., Halpern, J., 2014, *ApJ*, **793**, 78

Stappers, B. W., van Kerkwijk, M. H., Bell, J. F., Kulkarni, S. R., 2001, *ApJ*, **548**, L183

Thorstensen, J. R. & Armstrong, E., 2005, *AJ*, **130**, 759

Acknowledgement: I would like to thank Dr. John Antoniadis from the Dunlap Institute for Astronomy and Astrophysics, University of Toronto, for his friendly support and helpful discussions.

Additional tables and plots

Table 1. Parameters for PSR J1723−2837 [Crawford et al. 2013].

Parameter	**Value**
Right ascension (J2000)	17:23:23.1856(8)
Declination (J2000)	−28:37:57.17(11)
Spin frequency, f (s^{-1})	538.870683485(3)
Timing epoch (MJD)	55667
Time of ascending node, T_{asc} (MJD)	55425.320466(2)
Projected semi-major axis, x (s) [a]	1.225807(9)
Orbital frequency, f_b (s^{-1})	$1.88062856(2) \times 10^{-5}$
Orbital frequency derivative, $\dot{f}_b$ (s^{-2})	$1.24(4) \times 10^{-18}$
Orbital frequency second derivative, , $\ddot{f}_b$ (s^{-3})	$-2.6(3) \times 10^{-26}$
Spin period, P (ms)	1.855732795728(8)
Orbital period, Pb (d)	0.615436473(8)
Companion mass range ($M_\odot$)[d] 0.4−0.7	0.4−0.7
Orbital inclination angle range (degrees)[d]	30−41
Distance, d (kpc) [f]	0.75(10)

$a_x = a \sin i/c$ where a is the semi-major axis and i is the orbital inclination angle.

Table 2: A summary of the groups

GROUP	ACTIVITY	DATE	Observational Time window in days	DATA SETS (Night of observations)
1	**STABLE PERIOD** Ellipsoidal variation *(see figure 2)*	3 Aug – 1 Sep 2014	29	1-12 (12)
2	**UNSTABLE** Increase in flux at $\phi = 0.5$ *(see figure 3)*	12 Sep – 20 Oct 2014	38	13-25 (13)
BELOW NIGHT HORIZON				
3	**STABLE PERIOD** Ellipsoidal variation *(see figure 2)*	21 Mar – 18 Apr 2015	28	26-30 (5)
4	**UNSTABLE** Drop in flux Dips in Light Curve *(See figures 4 and 7–16)*			
5		19 May – 27 May 2015	8	35-37 (3)
6		06 Jun – 12 Jun 2015	6	38-42 (5)
7		19 Jun – 23 Jun 2015	4	43-46 (4)
8		12 Jul – 18 Jul 2015	6	47-50 (4)

9		25 Jul – 26 Jul 2015	1	51-52 (2)
10		04 Aug – 07 Aug 2015	4	53-56 (4)
11		02 Sep – 04 Sep 2015	2	57-59 (3)
12		18 Sep – 18 Sep 2015	1	60 (1)
13		19 Sep – 24 Sep 2015	6	61-62 (2)
14		30 Sep – 16 Oct 2015	17	63-68(6)

Table 3: Additional data on the observed dips.

GROUP	CENTRE DATE	Acc Days	Phase	Magnitde (Flat top)	Size (factor)
GRP 5	21-May-15	0.00	**0.76**	-0.050	1.20
GRP 6	9-Jun-15	19.00	0.70	-0.030	1.20
GRP 7	21-Jun-15	31.00	0.63	-0.030	1.20
GRP 8	15-Jul-15	55.00	0.28	-0.015	1.20
GRP 9	26-Jul-15	66.00	0.23	0.010	1.00
GRP 10	6-Aug-15	77.00	0.17	-0.025	1.10
GRP 11	3-Sep-15	105.00	-0.21	-0.035	1.10
GRP 12	18-Sep-15	120.00	**-0.24**	-0.025	1.50
GRP 13	22-Sep-15	124.00	-0.28	-0.050	1.40
GRP 14	8-Oct-15	140.00	-0.38	-0.050	1.50

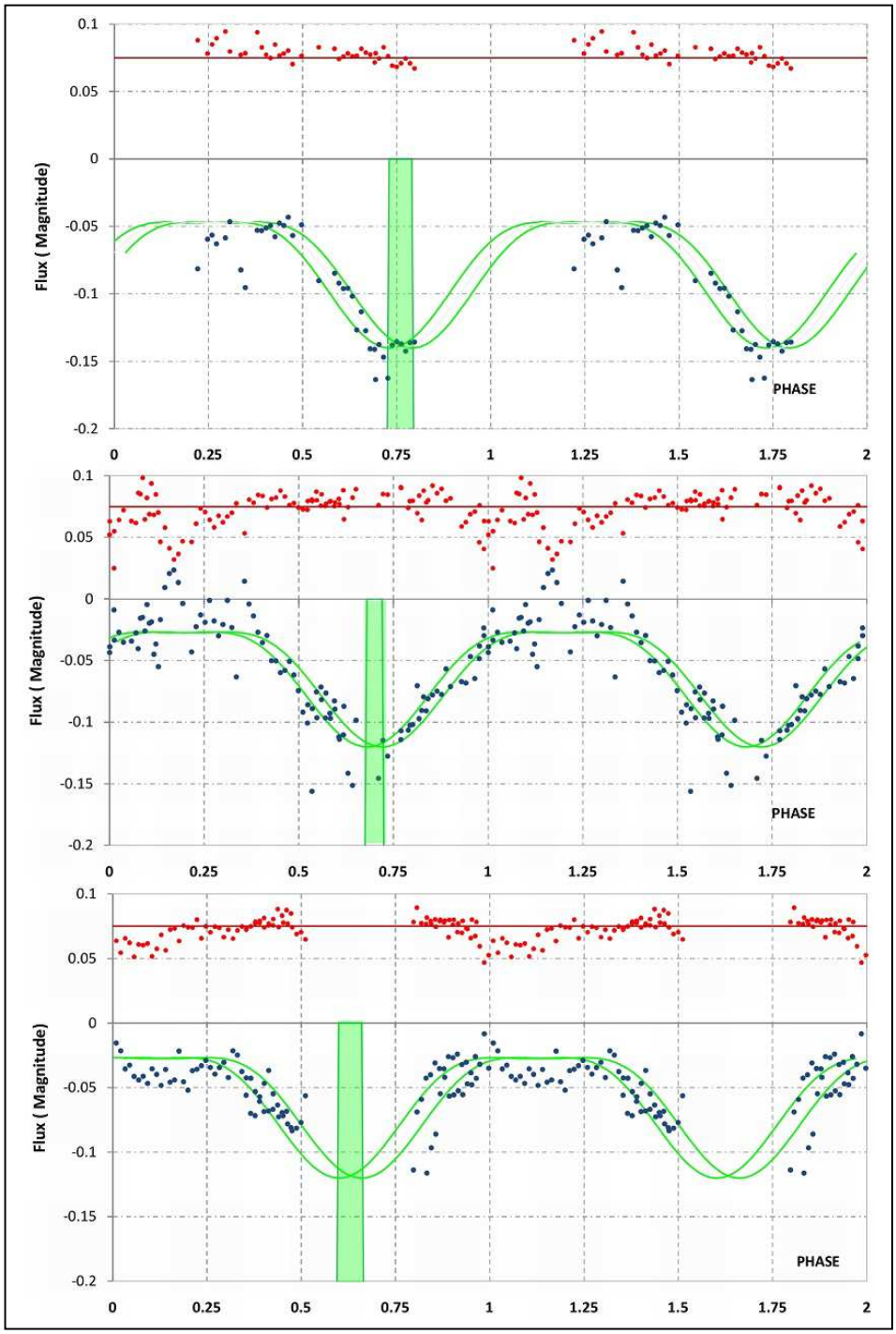

Figure 7, 8 & 9**:** *Folded light curve phase plots for J1723-2837 and the comparison star plotted on the same scale. From top to bottom are groups 5,6 & 7. Blue dots = J1723-2837. Red dots = comparison star. Green curves are nominal dip profiles to estimate the longitudinal centers. The green bars represent the centers of the dips while the widths of the bars are error estimates.*

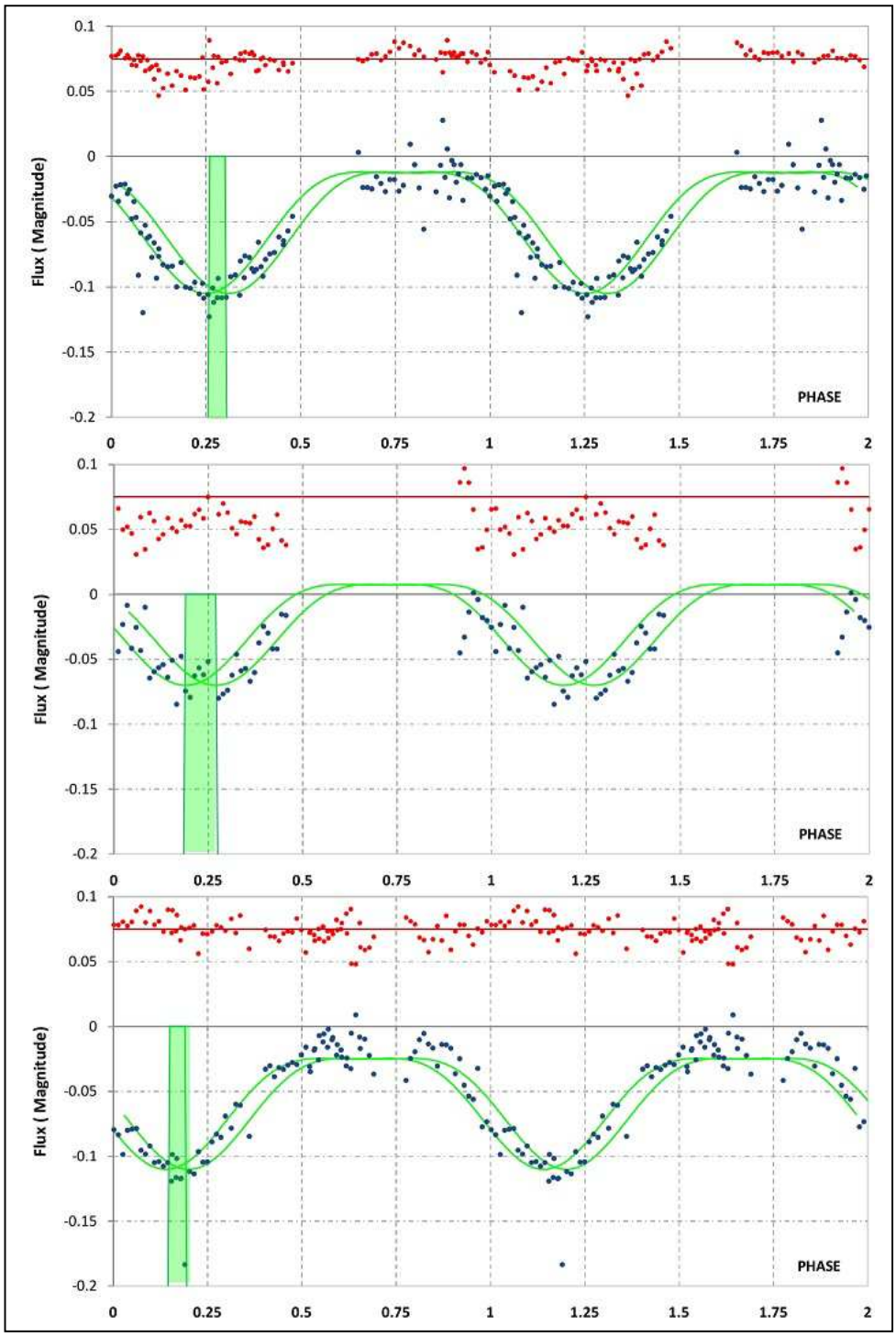

Figure 10, 11 & 12: *Folded light curve phase plots for J1723-2837 and the comparison star plotted on the same scale. From top to bottom are groups 8,9 & 10. Blue dots = J1723-2837. Red dots = comparison star. Green curves are nominal dip profiles to estimate the longitudinal centers. The green bars represent the centers of the dips while the widths of the bars are error estimates.*

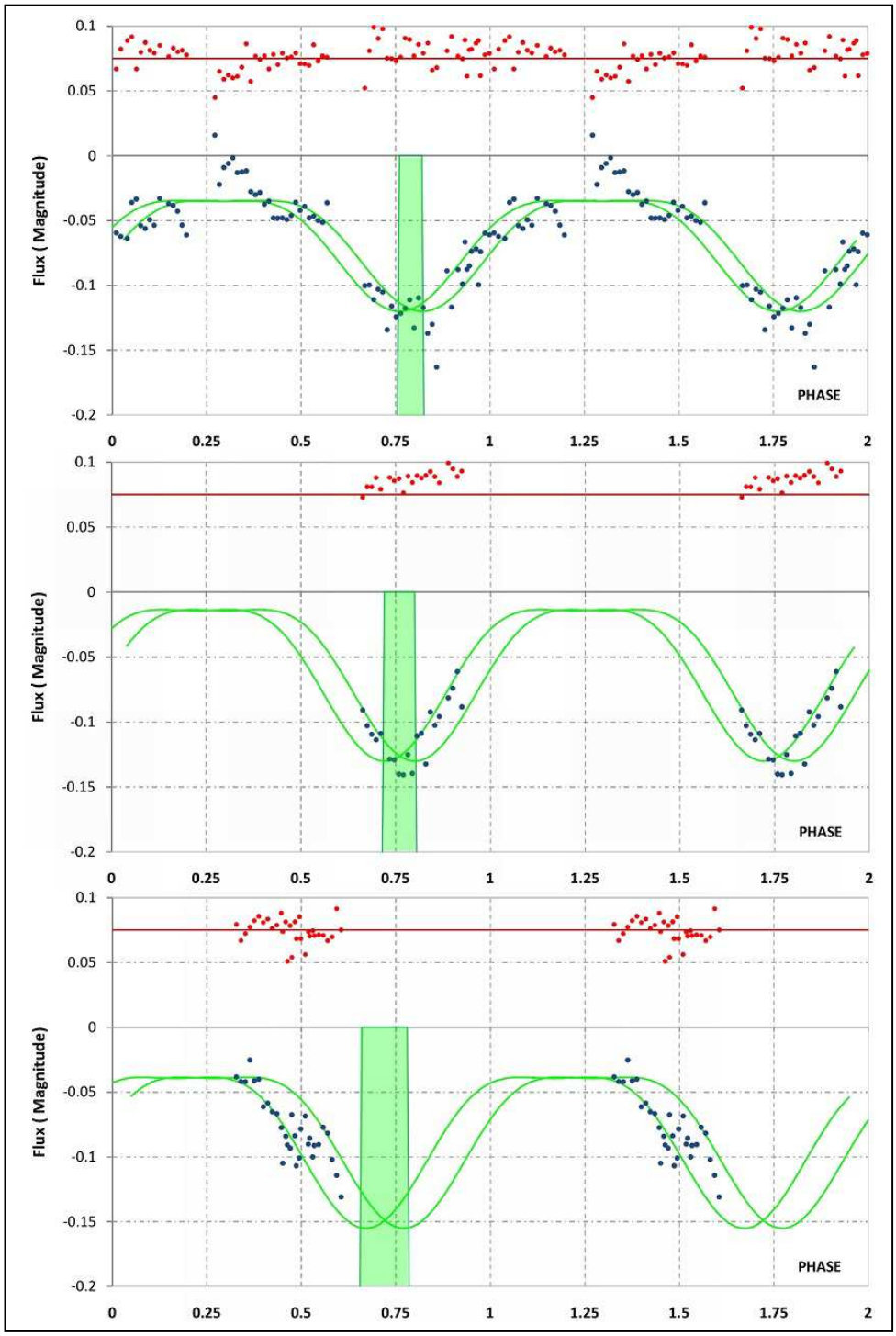

Figure 13, 14 & 15*: Folded light curve phase plots for J1723-2837 and the comparison star plotted on the same scale. From top to bottom are groups 11,12 & 13. Blue dots = J1723-2837. Red dots = comparison star. Green curves are nominal dip profiles to estimate the longitudinal centers. The green bars represent the centers of the dips while the widths of the bars are error estimates.*

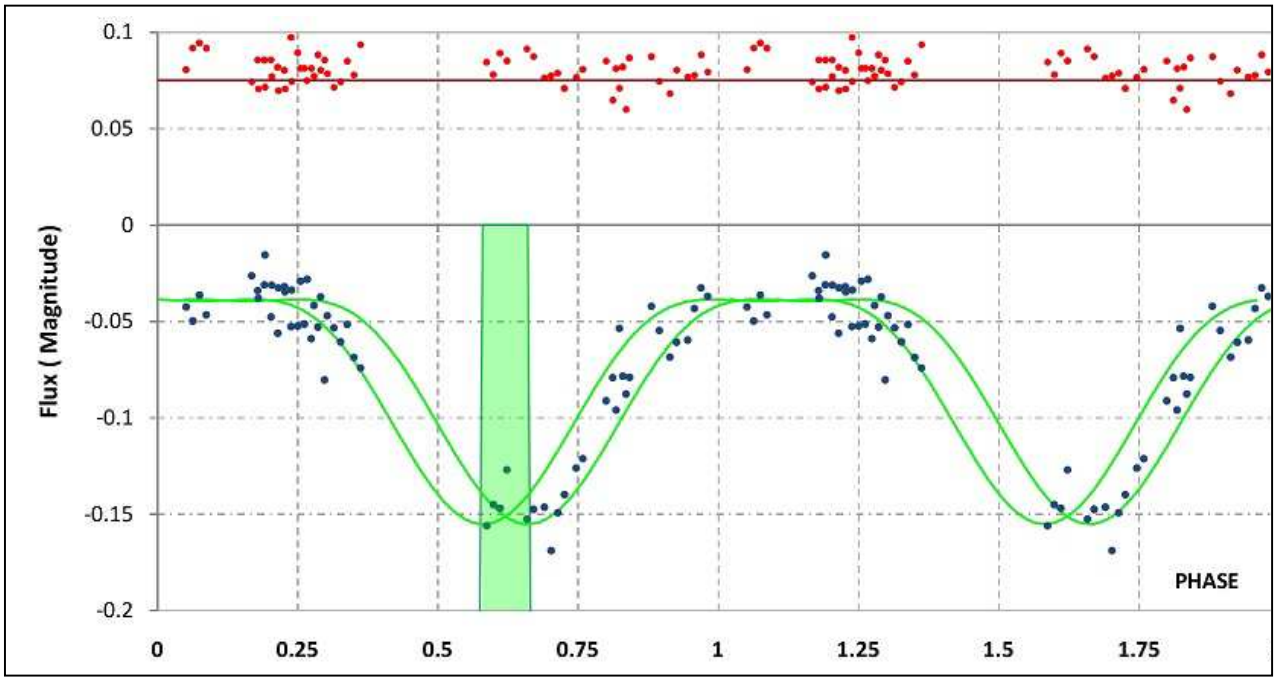

Figure 16 (GROUP 14)*: Folded light curve phase plot for J1723-2837 and the comparison star plotted on the same scale. Blue dots = J1723-2837. Red dots = comparison star. Green curves are nominal dip profiles to estimate the longitudinal centers. The green bars represent the centers of the dips while the widths of the bars are error estimates.*